ORCID:
ASB: 0000-0002-5884-0278
HQ: 0000-0002-3068-0313
GA: 0000-0002-9619-8538
AMA: 0009-0002-7822-9537
FAS: 0000-0002-5017-3570
MAZ: 0000-0003-0781-0121

Research Papers

Evaluation of silver nanoparticle antifungal activity biosynthesized from *Nigella sativa* extract, against *Aspergillus* species

Abdulrahman S. Bazaid[1,2,*], Husam Qanash[1,2], Ghaida Alsaif[1,2], Ali Saud Almalaq[1,2], Sghair Al-Kaseb[1,2], Ahmed M. Abdulfattah[3,4], Mohammed F. Abuzinadah[3,4], Faisal Al-Sarraj[5], Majid Al-Zahrani[6]

[1] Department of Medical Laboratory Science, College of Applied Medical Sciences, University of Ha'il, Hail 55476, Saudi Arabia
[2] Medical and Diagnostic Research Center, University of Ha'il, Hail 55473, Saudi Arabia
[3] Department of Medical Laboratory Sciences, Faculty of Applied Medical Sciences, King Abdulaziz University, Jeddah 21589, Saudi Arabia
[4] Embryonic Stem Cell Unit, King Fahd Medical Research Center, King Abdulaziz University, Jeddah 21589, Saudi Arabia
[5] Department of Biological Sciences, Faculty of Science, King Abdulaziz University, P.O. Box 80203, Jeddah,21589, Saudi Arabia
[6] Biological Science Department, College of Science and Art, King Abdulaziz University, Rabigh, Saudi Arabia
*Corresponding author. E-mail: ar.bazaid@uoh.edu.sa

Summary. Addressing emergent antifungal resistance associated with *Aspergillus* species and public health concerns posed by aflatoxin contamination requires new antifungal strategies. *Nigella sativa* (black seed) has shown promise when integrated with nanotechnology, making it a candidate for reducing aflatoxin risks. Antifungal activity of silver nanoparticles (AgNPs) synthesized using *N. sativa* was assessed against pathogenic *Aspergillus* species, and AgNP effects were assessed on expression of fungal genes related to toxin biosynthesis, membrane integrity, oxidative stress, and apoptosis. Silver nanoparticles were synthesized using aqueous extracts from *N. sativa*, and were spectroscopically characterized, confirming the functional groups involved in nanoparticle stabilization. Antifungal activity and gene expression were demonstrated *in vitro* and *in vivo* against *Aspergillus flavus*, *A. fumigatus*, and *A. niger*. The Ag-NPs biosynthesized by *N. sativa* had antifungal activity (MICs = 40–60 µg mL-1; MFCs = 90–120 µg mL^{-1}), and *A. fumigatus* was the most sensitive strain. Downregulation of aflR was reduced by 68% in *A. flavus*, erg11 by 42–55% in the three fungi, and catA was upregulated by 85–110%. These results indicate that Ag-NPs derived from *N. sativa* exert antifungal activity against *Aspergillus* species by at least two actions, suppression of aflatoxin biosynthesis and antifungal activity. This nanotechnology approach offers promise as a safe and effective alternative to traditional fungicide medications, which requires further in vivo evaluation.

Keywords. Aflatoxin, ergosterol, RT-PCR.

INTRODUCTION

Mycotic infections are important in human and animal health and agriculture, particularly those caused by *Aspergillus* spp., which are important fungal pathogens. The most common and invasive species are *A. flavus*, *A. fumigatus*, and *A. niger*. These species are also plant pathogens, infecting agricultural crops both in the field and post-harvest. These fungi infect different crops and human foods, and contaminate food with mycotoxins (Zakaria, 2024). Aflatoxins, primarily associated with *A. flavus*, are the most potent natural carcinogens, causing immunosuppression, liver cancer and growth retardation in humans and animals (Mallmann *et al.*, 2015; Awuchi *et al.*, 2021).

Current antifungal treatments mostly rely on chemical compounds that target fungal cells through various mechanisms, including azoles, which inhibit ergosterol synthesis,echinocandins, which disrupt cell wall formation, and polyenes, which damage membrane-bound structures. Despite these options, treating fungal infections remains challenging due to increasing drug resistance, high cost of treatments, potential drug toxicity, and narrow ranges of effectiveness of available medications (Gupta and Tomas, 2003; Berger *et al.*, 2017; Machado *et al.*, 2017).

Azoles, polyenes, and echinocandins are the primary fungicides used, although there is increasing concern due to the increasing resistance in pathogens to these treatments which weakens treatment strategies and increases requirement for development of new antifungal compounds (Gupta and Tomas, 2003; Machado *et al.*, 2017). Alongside human medicine, application of chemical fungicides has contributed to the development of pathogenic fungi that are resistant to these compounds, along with other ecological problems (Atanda *et al.*, 2005; Berger *et al.*, 2017).

Research has shown that common fungal infections, especially those caused by *Aspergillus*, are becoming increasingly difficult to treat with the usually used azoles (Gupta and Tomas, 2003). In agronomy, overuse of fungicides such as triazoles and benzimidazoles has led to emergence of resistant fungal strains, and has contributed to environmental pollution, posing potential human health risks (Berger *et al.*, 2017; Machado *et al.*, 2017).

For these reasons herbal plants are becoming popular as sources for new medicines that have antimicrobial and antifungal properties. *Nigella sativa* (black cumin) is a traditional herb that is widely used in Egypt and other regions. This plant has pharmacological properties including antimicrobial, antioxidant, anti-inflammatory, anticancer, and immunomodulatory effects (Vijayaku-

mar *et al.*, 2021; Mossa *et al.*, 2023; Abbas *et al.*, 2024). The seeds of *N. sativa* are rich in bioactive compounds including thymoquinone, p-cymene, carvacrol, thymohydroquinone, and flavonoids, which are medicinally important (Vijayakumar *et al.*, 2021; Abbas *et al.*, 2024).

Research has shown that phytochemicals of *N. sativa* are active against a range of gram negative and gram positive bacteria, viruses and fungi (Mossa *et al.*, 2023; Abbas *et al.*, 2024), and antifungal properties of these compounds have been reported against filamentous fungi, including *Aspergillus* spp. (Vijayakumar *et al.*, 2021; Mossa *et al.*, 2023). The phytochemicals of *N. sativa* disrupt microbial cell membranes and metabolism, and cause oxidative stress which has antimicrobial effects (Abbas *et al.*, 2024).

Nanotechnology offers effective methods for enhancing the antimicrobial properties of plant-based compounds. The antifungal activity of silver nanoparticles (AgNPs) has gained particular attention because of their multiple antimicrobial properties (Franci *et al.*, 2015; Gholamnezhad *et al.*, 2016). Synthesis of AgNPs using plant extracts ("biogenic synthesis,") is beneficial when compared to physical and chemical syntheses, because it is economical, environmentally-friendly, and the particles are biologically active (Gopinath *et al.*, 2017; Vijayakumar *et al.*, 2021; El-Seedi *et al.*, 2024; Pirbalouti *et al.*, 2024; Badmos et al., 2025). AgNPs can be synthesized from various plant extracts (Mallmann *et al.*, 2015; Gibała *et al.*, 2021; Hashem *et al.*, 2022; Pirbalouti *et al.*, 2024). These plant-mediated AgNPs contain silver ions which are combined with bioactive molecules from plants (El-Seedi *et al.*, 2024).

Although research has examined the use of AgNPs as antifungal agents, their molecular mechanisms of action against fungi have not been elucidated. Important molecular markers for antifungal action include the aflatoxin regulatory gene *aflR*, *erg11* which encodes lanosterol 14α-demethylase involved in ergosterol biosynthesis, and *catA* the oxidative stress contributing catalase gene. These genes are useful for probing antifungal responses in fungi (Deabes *et al.*, 2018; Peng *et al.*, 2018).

Downregulation of *aflR* probably causes aflatoxin production to be blocked. Similarly, suppressing *erg11* probably disrupts ergosterol biosynthesis, which is a key membrane component in fungi. Upregulation of *catA* may result in increased nanoparticle exposure and heightened oxidative stress (Franci *et al.*, 2015). RT-PCR allows monitoring of changes in gene expression in fungi due to treatments with antifungal agents, thus enabling real time tracking of gene expression changes in these organisms.

The present study has addressed two major problems: the growing resistance of *Aspergillus* species to

antifungal compounds, and the dangers posed by aflatoxins. By observing molecular markers, this research aimed to determine how AgNPs synthesized from *N. sativa* exert antifungal effects. This knowledge could allow the design of new and safe antifungal therapies.

MATERIALS AND METHODS

Preparation of Nigella sativa *extract*

Nigella sativa seeds were procured from a certified herbal outlet in Alexandria, Egypt. The seeds were washed with distilled water and air dried at room temperature (25 ± 2°C), then finely ground using a laboratory grinder. An extraction was carried out from 10 g of powdered seeds, using 100 mL of double distilled water, which was stirred continuously at 60°C for 60 min. The mixture was then filtered through Whatman No.1 filter paper, and the clear filtrate was kept at 4°C until used for nanoparticle synthesis.

Biosynthesis of silver nanoparticles

The green synthesis was performed by mixing 10 mL of the aqueous extract of *N. sativa* with 90 mL of 1mM solution of silver nitrate ($AgNO_3$) in sterile tubes. The reaction mixture was incubated at room temperature (25°C) in the dark with 150 rpm shaking for 24 h. The silver nanoparticles were visually confirmed by colour change from pale yellow to dark brown (Figure 1), which indicates surface plasmon resonance (SPR) of silver nanoparticles (Ahmed *et al.*, 2016).

The synthesized nanoparticles were collected and concentrated by centrifugation at 12,000 rpm for 15 min. They were then washed three times with distilled water plus ethanol to remove unreacted residues, and were then dried in a vacuum desiccator. The dried nanoparticles were stored in sterile containers at 4°C, until characterization and bioactivity assessments were carried out.

Characterization of synthesized silver nanoparticles

The biosynthesized silver nanoparticles were characterized using the following techniques:

UV–Visible spectroscopy. Absorption spectra within the range of 300–700 nm were recorded on a UV-Vis spectrophotometer (Shimadzu), for confirmation of nanoparticle synthesis and stability.

Fourier Transform Infrared Spectroscopy (FTIR). FTIR was used to detect functional groups for reduction and stabilization of the biosynthesized nanoparticles. The dried nanoparticle powder was mixed with potassium bromide (KBr) in a 1:100 ratio, and a Shimadzu FTIR (Shimadzu 8400S) spectrophotometer was used to scan the resulting spectra. The resulting FTIR spectrum was scanned in wave numbers from 500 cm^{-1} to 4000 cm^{-1}.

X-ray Diffraction (XRD). The crystallinity of the nanoparticles was assessed by recording of XRD patterns.

Transmission Electron Microscopy. Morphology, size and shape of the selenium nanoparticles were analyzed using a transmission electron microscope (TEM) (JEOL model JEM-2100), The aqueous suspension of AgNPs was ultrasonically dispersed, and the sample was prepared by adding a drop of the suspension onto a carbon-coated copper grid, and this was then dried using an IR lamp. Micrographs were capture using 80 kV accelerating voltage. The pattern of size distribution for the particles was determined by measuring and counting of 200 separate particles from TEM images.

Fungus cultivation and inoculum preparation

A collection of previously identified fungi was provided by Dr Elsayed Shabaan, Plant Protection and Biodiagnostics Department, Arid Land Cultivation Research Institute (ALCRI), City of Scientific Research and Technological Applications (SRTA-CITY), Alexandria, Egypt. This included *Aspergillus flavus* (KJ831193), *Aspergillus fumigatus* (KJ831194), and *Aspergillus niger* (ATCC 16888).

The *Aspergillus* species were grown on Sabouraud Dextrose Agar (SDA) plates for 5 to 7 d at 28°C. Resulting conidia were collected by rinsing the plates with sterile saline containing 0.1% Tween 80, which was then filtered through sterile gauze to remove mycelium debris. Using a hemocytometer, the conidium concentration was adjusted to 1×10^6 conidia mL^{-1}.

Figure 1. The synthesized silver nanoparticles showed a dark colour in solution (left).

In vitro *assessments of antifungal activity*

Disk diffusion assay

Based on CLSI M38-A2 guidelines (Clinical and Laboratory Standards Institute, 2015), the antifungal activity of the synthesized AgNP was assessed using the disk diffusion method. Fungal spore suspension (100 µL) was evenly spread on the surface of each SDA plate. Sterile paper disks (6 mm diam.) previously loaded with 50 µL of AgNPs at concentrations between 25 and 200 µg mL^{-1} were then placed on the inoculated plates. The plates were then incubated at 28°C for 48 h, after which resulting zones of inhibition were measured.

Minimum Inhibitory Concentrations (MIC) and Minimum Fungicidal Concentrations (MFC)

MICs and MFCs were analyzed using the broth microdilution method, following CLSI guidelines (M38-A2). In 96-well microtiter plates containing Sabouraud Dextrose Broth (SDB), two-fold serial dilutions of AgNPs (from 5 to 200 µg mL^{-1}) were prepared. Each well was then inoculated with 100 µL of conidium suspension (1×10^4 conidia mL^{-1}). The plates were then incubated at 28°C for 48 h. The MIC was defined as the lowest AgNP concentration at which no fungal growth was observed. For MFC determination, aliquots (as above) were sub-cultured onto SDA plates, and the lowest concentration at which no fungal colonies were observed after 72 h incubation at 28°C was recorded as the MFC.

Bioactive compound analysis using GC-MS

A Gas Chromatography-Mass Spectrometry (GC-MS) analysis was carried out to identify the phytochemical constituents responsible for antifungal activities of *N. sativa* extract. Chemical profiling of *N. sativa* aqueous extract was carried out after freeze-drying to yield a 10 mL portion. This was re-dissolved in 2 mL of methanol, and the solution was filtered using a 0.22 µm syringe filter. The solution was then analyzed using a GC-MS system (Agilent 7890A) with a 5975C MS detector. The separation was carried out in an HP-5MS capillary column (30 m × 0.25 mm, 0.25 µm film thickness). The oven temperature was set to rise from 60°C (3 min hold) to 280°C with a ramp of 10°C min^{-1}. The carrier gas was helium with constant flow of 1.0 mL min^{-1}, the injector was set at 250°C, and a volume of 1 µL was used for injection in splitless mode. Mass spectra were collected in EI mode at 70 eV. Items in the sample were identified from elative indices and mass spectra (RI-MS) matching against WILEY and National Institute of Standards and Technology (NIST08) library data (http://webbook.nist.gov; accessed 20 November 2021), supplied with the computer-controlled GC-MS system.

RNA extraction and cDNA synthesis

Aspergillus cultures were treated with sub-inhibitory concentrations of AgNPs (at MIC/2), and were then incubated for 24 h. Total RNA was extracted from treated and untreated cultures using TRIzol reagent (Invitrogen). RNA purity and concentrations were assessed using NanoDrop spectrophotometry (Thermo Fisher Scientific). High-quality RNA (A260/A280 ratio between 1.8 and 2.0) underwent cDNA synthesis using the RevertAid First Strand cDNA Synthesis Kit (Thermo Fisher Scientific).

Real-Time quantitative PCR (RT-qPCR)

Expressions of *aflR*, *erg11*, and catA genes were analyzed using RT-qPCR with SYBR Green detection on an Applied Biosystems StepOnePlus Real-Time PCR System (Thermo Fisher Scientific). Each reaction contained 10 µL of SYBR Green Master Mix, 1 µL each of forward and reverse primers (10 µM), 2 µL of cDNA template, and 6 µL of nuclease free water, in a total volume of 20 µL. The β-actin gene was used as an internal control. The thermal cycling conditions were as follows: initial denaturation at 95°C for 5 min; 40 cycles each of denaturation at 95°C for 15 sec, annealing at 60°C for 30 sec, and extension at 72°C for 30 sec. All reactions were carried out in triplicate. Relative gene expression was calculated using the 2^−ΔΔCt method (Livak and Schmittgen, 2001).

In planta *biocontrol assay using banana tissue culture*

Banana plantlets (*Musa* spp.) were used for the *in planta* assay, to replicate post-harvest scenarios where *A. flavus* is known to grow on a variety of fruits and stored foods which are left unprotected. The technique using banana tissue culture allows for the observation of fungal colonization and antifungal activity under conditions of fungal infection devoid of contamination, using a standardized tissue culture method. *Aspergillus flavus* is not a classical pathogen of the banana, yet, in the present study experiments, banana plantlets inoculated with this fungus exhibited chlorosis, necrosis and browning at

the bases of pseudostems. This model system provided a repeatable process for determining *in planta* biocontrol activity of AgNPs against *A. flavus*. An *in vitro* assay to test the antifungal activity of *N. sativa*-mediated AgNPs was also carried out using sterile tissue cultured banana plantlets (*Musa* spp.).

Banana shoot tips were procured from healthy suckers and were surface sterilized using 70% ethanol for 1 min followed by 20% sodium hypochlorite for 15 min, and then rinsing three times in sterilized distilled water. The explants were then inoculated onto Murashige and Skoog (MS) medium containing 3% sucrose and 2 mg L^{-1} 6-benzylaminopurine (BAP), for shoot multiplication. The shoots were then incubated at 25°C in 16 h light/8 h darkness. After 3 weeks, healthy banana plantlets were each inoculated at the pseudostem base with 10 µL of *A. flavus* conidium suspension (1×10^6 conidia L^{-1}), using a sterile micropipette. Inoculated plants were then maintained for 24 h before interventions were made. AgNPs were administered through a sterile micropipette tip just proximal to the *A. flavus* inoculation sites.

Experimental designs

The experiments were of randomized layouts. For all *in vitro* analyses (disk diffusion, MIC, and MFC), treatments were applied in a fully random fashion across microtiter plates and culture dishes. Each treatment was applied to three independent biological replicates, each of which had three technical repeats. For the *in planta* banana experiment, plantlets were randomly assigned to treatment groups (infected only, infected + 50 µg mL^{-1} AgNPs, infected + 100 µg mL^{-1} AgNPs). Each treatment group consisted of ten plantlets, and the experiment was independently conducted twice. The following parameters were recorded at 7 d following treatments: symptom scoring (yellowing and necrosis) on a 0 to 5 scale; fungal re-isolation on PDA to confirm colonization; tissue aflatoxin B1 quantification by ELISA; and photographic documentation of disease phenotypes.

Statistical analyses

All data were analyzed using SPSS software (Version 22.0; IBM Corp.). Results were expressed as means ± standard deviations (SD). Differences between treated and control groups were analyzed using Student's t-test at $P < 0.05$. Mean values, each from two replicates, were recorded.

RESULTS

GC-MS profile of Nigella sativa *extract*

Analysis by GC-MS of the aqueous extract from *N. sativa* showed several bioactive compounds. The most important constituents are described in Table 1.

Characterization of biosynthesized silver nanoparticles

The successful synthesis of AgNPs using *N. sativa* extract was confirmed by multiple characterization techniques. UV-Visible Spectroscopy gave an absorption peak at 428 nm, indicating presence of surface plasmon resonance for silver ions, confirming formation of the AgNPs (Figure 2A). FTIR analysis showed characteristic peaks corresponding to -OH, C=O, and -NH bonds, indicating secondary metabolites responsible for stabilization of the nanoparticles (Figure 2B).

The AgNPs produced by the biological method were first examined by X-ray diffraction (XRD) (Figure 3). The resulting pattern had four sharp peaks with respective approx. 2θ values of 36°, 42°, 60°, and 74°. These correspond, respectively, to the (111), (200), (220), and (311) crystal planes of silver. These reflections confirm that the nanoparticles had a face-centered cubic (fcc) lattice, verifying that well-formed crystalline AgNPs had been synthesized. The strongest (111) peak indicates that most particles preferentially grew along this direction, a behaviour frequently observed in metal nanoparticles made with plant extracts.

Table 1. Major bioactive compounds identified from *Nigella sativa* using GC-MS.

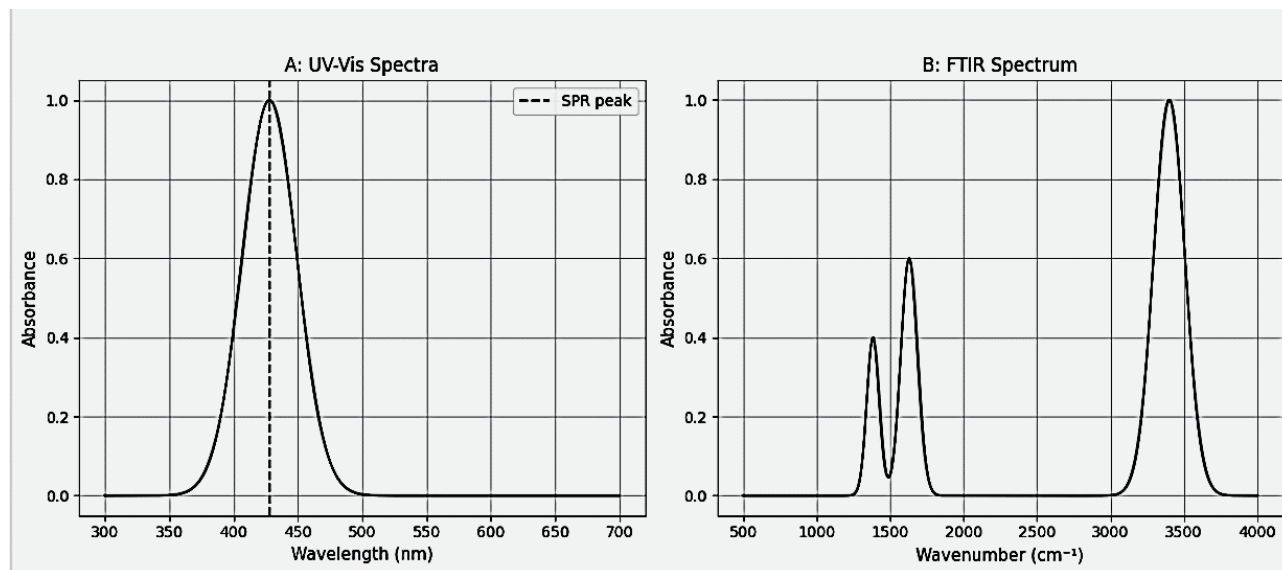| Mean retention time (min)	Compound name	Molecular formula	Mean peak area (%)	Reported biological activity	References
7.85	Thymoquinone	$C_{10}H_{12}O_2$	29.4	Antifungal, antioxidant, anti-inflammatory	Khader and Eckl (2014)
9.14	p-Cymene	$C_{10}H_{14}$	17.6	Antimicrobial, membrane disruption	Burt *et al.*, 2007
10.62	α-Thujene	$C_{10}H_{16}$	11.2	Antioxidant, antifungal	Kanika and Satyawati, (2022)
11.45	Carvacrol	$C_{10}H_{14}O$	9.8	Antifungal, anti-biofilm	Gómez-Sequeda *et al.*, (2020)
13.71	Thymol	$C_{10}H_{14}O$	6.3	Antiseptic, antifungal	Jung *et al.*, (2021)
16.27	Linoleic acid	$C_{18}H_{32}O_2$	5.1	Membrane disruption, anti-aflatoxin	Wu *et al.*, (2022)

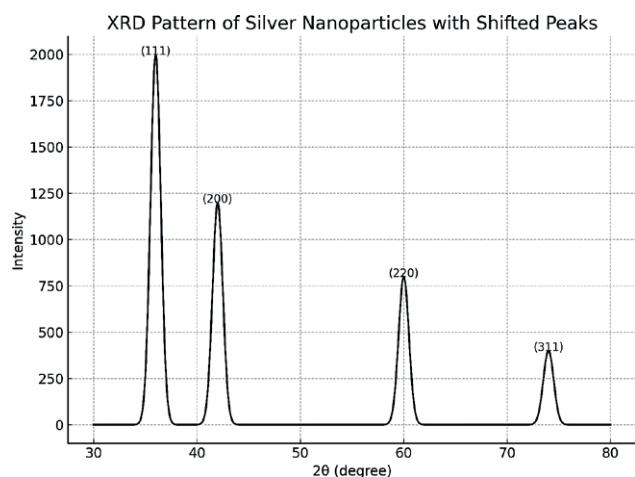**Figure 2.** Spectra for characterization of silver nanoparticles.

Figure 3. X-ray Diffraction (XRD) pattern for silver nanoparticles.

Figure 4. Nanoparticle sizes and shapes shown using transmission electron microscopy.

The minor shifts of the peaks away from standard positions probably arose from internal strain or small crystal size, features typical of biosyntheticized and low-temperature materials. No extra peaks appeared in the pattern, confirming that the product was phase-pure and free of detectable impurities from other silver allotropes.

TEM images (Figure 4) showed that the nanoparticles are mostly spherical or nearly so, and were evenly distributed with little clustering. Size annotations in Figure 4 indicate nanoparticle diameters from approx. 16.19 nm to 45.86 nm, affirming that the particles occupy the nanoscale needed for strong biological activity. This size range matches the histogram generated by image analy-sis software, which identified an average diameter of approx. 27 nm.
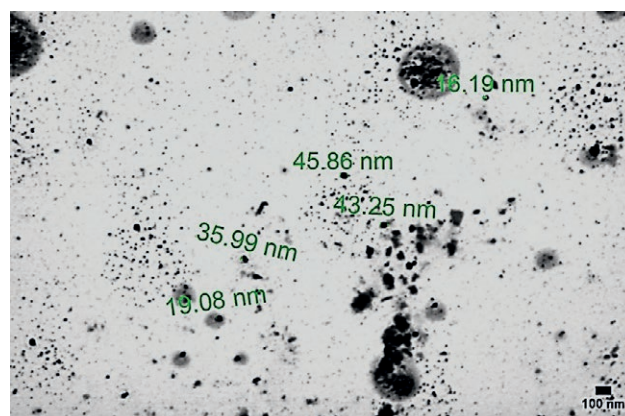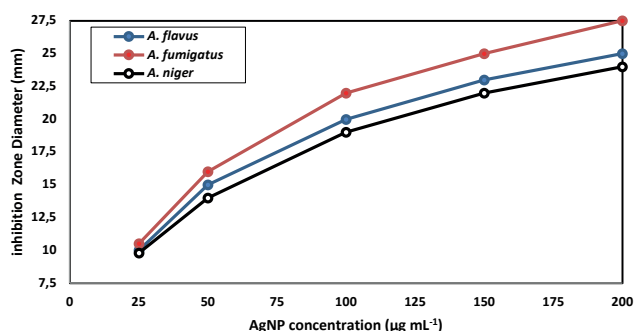
Antifungal activity of Nigella sativa-*mediated silver nano-particles*

Diameters of inhibition zones increased with increasing AgNP concentrations in a dose-dependent manner (Figure 5). The antifungal effects of the syn-thesized AgNPs on the isolates of *A. flavus, A. fumiga-tus,* and *A. niger* assessed in the disk diffusion, MIC and MFC assays are summarized in Table 2. *Aspergillus fumigatus* (KJ831194) was the most sensitive isolate to

Table 2. The minimum inhibitory concentrations (MIC) and minimum fungicidal concentrations (MFC) against three *Aspergillus* spp. isolates.

Fungus isolate	MIC (μg mL^{-1})	MFC (μg mL^{-1})
A. flavus (KJ831193)	50	100
A. fumigatus (KJ831194)	40	90
A. niger (ATCC 16888)	60	120

Figure 5. Mean diameters of culture inhibition zones for three Aspergillus spp. isolates grown in cultures containing different AgNP concentrations.

Table 3. Mean concentrations of aflatoxin B1 in banana plantlets treated with different amounts of AgNPs after inoculation with Aspergillus flavus.

Treatment	Mean aflatoxin B1 concentration (ppb)*
Inoculated only	142.7 ± 5.9
Inoculated, + 50 μg /mL^{-1} AgNPs	52.1 ± 3.4
Inoculated, + 100 μg mL^{-1} AgNPs	19.6 ± 2.8

*All differences in means were statistically significant ($P < 0.01$).

Figure 6. Banana plantlets treated with different concentrations of AgNPs.

AgNPs, while *A. niger* (ATCC 16888) had comparatively greater MIC and MFC values.
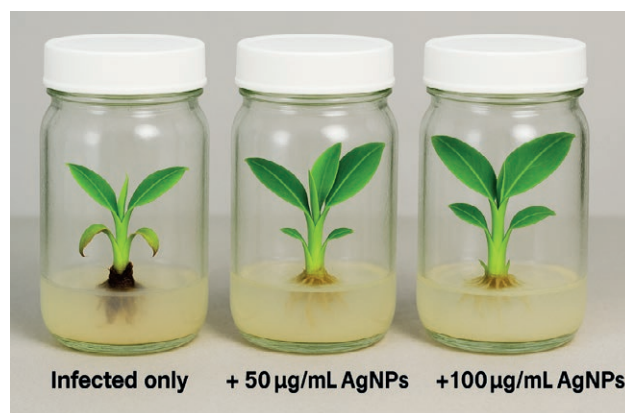
Antifungal effects on banana plantlets

Quantification of *in planta* fungus recovery relied on banana tissue colonization by *A. flavus* assessed from re-isolation frequency. A piece of surface sterilized pseudostem base tissue was removed from each plantlet at 1 week intervals, and *A. flavus* re-isolation frequency was determined on PDA plates. Each treatment yielding *A. flavus* was recorded and the frequency of recovery of *A. flavus* was computed (Figure 6). This metric, in conjunction with *A. flavus* sample populations, determined the degree of colonization and the effectiveness of AgNP treatment in mitigating fungal persistence.

In untreated cultures, *A. flavus* (KJ831193)-inoculated banana plantlets developed severe chloroses and pseudostem tissue browning necroses, with a mean symptom score of 4.5 ± 0.3. AgNP treatment induced a dose-dependent protective response. Plantlets treated with 50 μg mL^{-1} AgNPs had mild necroses, with a symptom score of 2.3 ± 0.4, while those treated with 100 μg mL^{-1} AgNPs displayed almost normal morphology, with a symptom score of 1.1 ± 0.3. Fungus re-isolations assays resulted in dense fungal growth from untreated samples, whereas plantlets treated with AgNPs gave reduced fungus recovery.

RT-qPCR gene expression results

Expression of genes related to aflatoxin biosynthesis (*aflR*), ergosterol synthesis (*erg11*), and oxidative stress response (*catA*) after treatment with sub-inhibitory concentrations (MIC/2) of AgNPs are summarized in Table 3. Figure 7 summarizes data of gene expression in response to the three *Aspergillus* spp. isolates.

After AgNPs treatment, *A. flavus* showed substantial downregulation of the *aflR* gene, which indicated reduced aflatoxin biosynthesis. The mean down regulation fold change was 0.32 (68% downregulation; $P < 0.01$).

Expression levels of the *erg11* gene were also downregulated in all three *Aspergillus* spp. isolates. This indicated disruption of ergosterol biosynthesis, which is important for structural integrity of fungal cell membranes. Mean downregulation fold changes were: for *A. flavus*, 0.45 (55% downregulation; $P < 0.01$); *A. fumigatus*, 0.52 (48% downregulation; $P < 0.01$), and for *A. niger*, 0.58 (42% downregulation; $P < 0.01$).
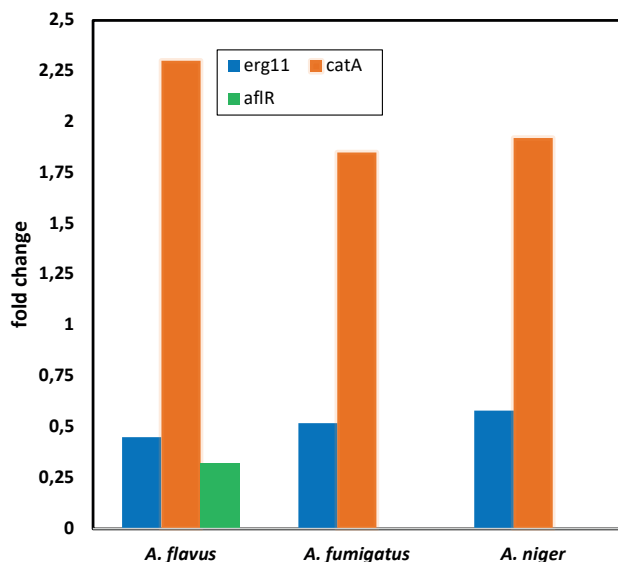
Figure 7. Mean expression fold changes for three genes in three Aspergillus species isolates, after AgNP treatments.

The stress response gene *catA* associated with oxidative stress was overexpressed in all three fungal species, indicating production of reactive oxygen species (ROS) due to the AgNPs. Mean fold changes were: *A. flavus*, 2.10 (110% upregulation; $P < 0.01$); *A. fumigatus*, 1.85 (85% upregulation; $P < 0.01$), and *A. niger*, 1.92 (92% upregulation; $P < 0.01$).

DISCUSSION

This study aimed to assess the potential antifungal activity of silver nanoparticles (AgNPs), synthesized using aqueous extract of *N. sativa*, against isolates of *A. flavus*, *A. fumigatus*, and *A. niger*. Pirbalouti *et al*., (2024) and Gopinath *et al*., (2017) reported that colour change from pale yellow to dark brown marked the initial stages in the synthesis of AgNPs, and indicated their formation. In the present study, XRD analyses did not detect extra peaks, verifying that the product obtained was phase-pure with no other impurities of other silver allotropes.

These results are similar to those in past reports of AgNP synthesis through *N. sativa* extracts (Vijayakumar *et al*., 2021; Mossa *et al*., 2023), and further indicate an environmentally acceptable route to quality silver crystallites. The AgNPs were confirmed to have been formed, as SPR peaks were recorded at 428 nm using UV-Vis spectrometry (Franci *et al*., 2015). FTIR analysis confirmed some functional groups as hydroxyl, carbonyl,

and amine groups. These probably arose from thymoquinone, flavonoids, and proteins in the extract from *N. sativa*, which served as the reducing and stabilizing agents (Vijayakumar *et al*., 2021; Abbas *et al*., 2024).

This method of biosynthesis fits with the principles of "green nanotechnology", which has garnered increasing attention due to emphasis on minimizing the use of toxic chemicals in production of nanoparticles (El-Seedi *et al*., 2024).

Results from the disk diffusion and MIC/MFC assays confirmed that all the assessed *Aspergillus* isolates were sensitive to the AgNPs, with activity being dose dependent. AgNP MIC values of 40-60 µg mL^{-1} and MFC values of 90-120 µg mL^{-1} are within ranges documented for silver nanoparticles synthesized from plant extracts (Mallmann *et al*., 2015; Hashem *et al*., 2022).

Among the three fungus isolates assessed, *A. fumigatus* displayed the greatest sensitivity, while *A. niger* showed the greatest MIC and MFC values, indicating species-dependent susceptibility. A diverse array of AgNP antifungal actions is probable, including disruption of membrane integrity of the fungus through generation of reactive oxygen species (ROS), blockage of essential metabolic pathways, and interference with DNA and protein synthesis (Franci *et al*., 2015; Gholamnezhad *et al*., 2016). Among the tested species, *A. fumigatus* had the greatest sensitivity to AgNP treatment, which could be due cell wall composition and membrane physiology of this fungus (Vanlalveni *et al*., 2024). Previous studies have shown that *A. fumigatus* has greater membrane permeability and thinner cell walls compared to other *Aspergillus* species, making it more vulnerable to nanoparticle penetration and oxidative stress. In addition, the downregulation of *erg11* observed in *A. fumigatus* suggests a strong disruption of ergosterol biosynthesis, which affects membrane stability and enhances antifungal susceptibility. These structural and molecular characteristics may explain why *A. fumigatus* responded more sensitively to AgNP exposure than *A. flavus* and *A. niger*.

These results align with previously reported synergistic effects of silver ions and *N. sativa* phytochemicals, which had strong antifungal activities. This indicates increased enhancement of bioactivity of the nanoparticles (Atanda *et al*., 2005; Badmos *et al*., 2025).

Further investigations of response of *Aspergillus* species to AgNP exposure could be conducted based on RT-qPCR outcomes. The pronounced downregulation of *aflR* in *A. flavus* signals disrupted aflatoxin biosynthesis, which confirms previous findings indicating nanoparticle treatments may reduce mycotoxin production (Deabes *et al*., 2018). The *aflR* blockade supports the assump-

tion that AgNPs could be utilized to mitigate risks of fungal mycotoxins in contaminated food products, to reduce the threats aflatoxin poses to food safety.

All three assessed *Aspergillus* species had *erg11* downregulation, indicating that AgNPs interfere with the ergosterol biosynthesis crucial for the structural integrity of the fungal cell membranes. Disruption of ergosterol synthesis is a well-documented antifungal mechanism, as occurs for azole compounds (Gupta and Tomas, 2003). AgNP induced downregulation of *erg11* has also been shown in other fungi (Deabes *et al*., 2018). Toxicity of AgNPs may also stem from their effects on the catalase enzyme, demonstrated in the upregulation of *catA*. More specifically, silver nanoparticles are well known for their powerful antifungal activity through cell wall and membrane destruction, generation of reactive oxygen species (ROS), interactions with important cellular macromolecules including DNA and proteins, and inhibition of key enzymes (Franci *et al*., 2015; Gholamnezhad *et al*., 2016).

The azole class of antifungal chemicals have induced development of resistance in fungi to these compounds, which created need for alternative therapies (Gupta and Tomas, 2003; Machado *et al*., 2017). The new "green-synthesized" AgNPs have multi-targeted mechanisms of action and low probability of inducing pathogen resistance, which is an advantage over previously developed antifungal chemicals (Deabes *et al*., 2018; El-Seedi *et al*., 2024).

Nigella sativa is also a safe plant, and may enhance biocompatibility along with stability of nanoparticles previously synthesized (Vijayakumar *et al*., 2021; Abbas *et al*., 2024).

Application of *N. sativa*-based AgNPs to combat *Aspergillus flavus* infections in horticultural systems has promise, as indicated by their activity in controlling infections in banana plantlets. Aflatoxins, especially those from *A. flavus*, are among the most toxic natural compounds. They can cause severe short- and long-term health problems in animals and humans (Mallmann *et al*., 2015; Awuchi *et al*., 2021). Aflatoxin is a widespread human and animal food safety issue, especially in tropical and subtropical regions (Atanda *et al*., 2005; Peng *et al*., 2018). Aflatoxin causes hepatocellular carcinoma, growth impairment, and immunosuppression from chronic exposure. The decrease in aflatoxin B1, along with reduced fungal growth and tissue damage, indicate that synthesized silver nanoparticles could provide effective biological control for toxin-producing fungi.

The tissue culture system used in the present study was chosen because it usually remains free of contaminants, thus providing a balanced environment to test the AgNP effectiveness on banana, which may be prone to postharvest mycotoxin development. Plant-based nanotechnology applied in agriculture is likely to broaden scope of the technology. Greenhouse and field experiments would be worthwhile to assess sprays and coatings of AgNPs on banana bunches for suppression of fruit pathogens.

Limitations in the scope of the present study are recognized. Only clinical and laboratory strains of *Aspergillus* spp. were used; responses from environmental isolates may differ from those recorded here. Safety, pharmacokinetics, and therapeutic efficacy of nanoparticles require validations through *in vivo* studies prior to clinical or agricultural uses. As well, evaluations are required to determine long-term stability, mammalian cell cytotoxicity, and potential environmental impacts of these materials (Gholamnezhad *et al*., 2016; Vignesh *et al*., 2025). Focus should also be directed at functionalization of nanoparticle surfaces, optimization of large-scale synthesis, and exploration of synergism of these materials with other antifungal agents.

CONCLUSIONS

The present study has indicated that AgNPs biosynthesized using aqueous extract from *N. sativa* had antifungal activity against *A. flavus*, *A. fumigatus*, and *A. niger*. The nanoparticles exerted dose-dependent antifungal effects causing inhibition in cultures, low MICs and MFCs, and suppression of fungal growth *in vitro*. At molecular level, RT-qPCR analysis showed that AgNP treatments downregulated genes responsible for aflatoxin biosynthesis and ergosterol, which are important aspects for sustaining activity and pathogenicity of these fungi. At the same time, the increase of *catA* suggests that AgNPs exert antifungal activity mainly through oxidative damage. This research provides knowledge supporting the "green synthesis" approach, which has ecological advantage, as it is low cost and is unlikely to cause environmental damage. The combined antimicrobial effect of *N. sativa* phytochemicals and silver nanoparticles may provide an effective alternative to conventional antifungal therapies. This research has contributed to nanobiocontrol, and particularly provides direction for addressing threats of antifungal resistance and aflatoxin contamination of foodstuffs.

Further research is required to make safety assessments, and assess practical applications, to tailor nanoparticle formulations for clinical and agricultural applications.

LITERATURE CITED

Abbas M., Gururani M.A., Ali A., Alsahli A.A., Almatroudi A., ….. El Ansari F., 2024. Antimicrobial properties and therapeutic potential of bioactive compounds in *Nigella sativa*: A review. *Molecules* 29(20): 4914. https://doi.org/10.3390/molecules29204914

Ahmed S., Ahmad M., Swami B.L., Ikram S., 2016. A review on plants extract mediated synthesis of silver nanoparticles for antimicrobial applications: A green expertise. *Journal of Advanced Research* 7(1): 17–28.

Atanda O.O., Akpan I., Rati E.R., Ozoje M., 2005. Palm kernel: A potential substrate for rapid detection of aflatoxin in agricultural commodities. *African Journal of Biotechnology* 5: 1029–1034.

Awuchi C.G., Echeta K.A., Ngwu E.K., Obayiuwana E., Amagwula I.O., Okpala C.O.R., 2021. Mycotoxins affecting animals, foods, humans, and plants: Types, occurrence, toxicities, action mechanisms, prevention, and detoxification strategies—A revisit. *Foods* 10(6): 1279.

Badmos A., Oni E., Ojewale I., Oluwafemi F., 2025. Evaluating the potency of Nigella sativa-mediated silver nanoparticles against aflatoxigenic fungi in planting soil. *Food and Environment Safety* 24(1): 33–44. https://doi.org/10.4316/fens.2025.004

Berger S., El Chazli Y., Babu A.F. and Coste A.T., 2017. Azole Resistance in *Aspergillus fumigatus*: A Consequence of Antifungal Use in Agriculture? *Frontier of Microbiology* 8: 1024. https://doi.org/10.3389/fmicb.2017.01024

Burt S.A., Van Der Zee R., Koets A.P., De Graaff A.M., Van Knapen F., … Veldhuizen E.J.A., 2007. Carvacrol induces heat shock protein 60 and inhibits synthesis of flagellin in *Escherichia coli* O157:H7. *Applied and Environmental Microbiology* 73: 4484–4490. https://doi.org/10.1128/AEM.00340-07.

Clinical and Laboratory Standards Institute (CLSI), 2015. *Performance Standards for Antimicrobial Disk Susceptibility Tests; Approved Standard - Twelfth Edition* M02- A12., CLSI, (ISBN 1-56238-985-8 (print); ISBN 1-56238-986-6 (Electronic). Clinical and Laboratory Standards Institute, 950 West Valley Road, Suite 2500, Wayne, PA, 19087 USA.

Deabes M.M., Khalil W.K.B., Attallah A.G., El-Desouky T.A., Naguib K.M., 2018. Impact of Silver Nanoparticles on Gene Expression in *Aspergillus flavus* Producer Aflatoxin B1. *Open Access Macedonian Journal of Medical Sciences* 6(4): 600–605. https://doi.org/10.3889/oamjms.2018.117

El-Seedi H.R., Omara M.S., Omar A.H., Elakshar M.M., Shoukhba Y.M., … S. A. M. Khalifa, 2024. Updated Review of Metal Nanoparticles Fabricated by Green Chemistry Using Natural Extracts: Biosynthesis, Mechanisms, and Applications. *Bioengineering* 11: 1095. https://doi.org/10.3390/bioengineering11111095

Franci G., Falanga A., Galdiero S., Palomba L., Rai M., ….. Galdiero M., 2015. Silver nanoparticles as potential antibacterial agents. *Molecules* 18: 20(5): 8856–8874. https://doi.org/10.3390/molecules20058856.

Gholamnezhad Z., Havakhah S., Boskabady M.H., 2016. Preclinical and clinical effects of *Nigella sativa* and its constituent, thymoquinone: A review. *Journal of Ethnopharmacology* 22(190): 372–386. https://doi.org/10.1016/j.jep.2016.06.061

Gibała A., Żeliszewska P., Gosiewski T., Krawczyk A., Duraczyńska D., …. Oćwieja M., 2021. Antibacterial and antifungal properties of silver nanoparticles-effect of a surface-stabilizing agent. *Biomolecules* 7: 11(10): 1481. https://doi.org/10.3390/biom11101481 PMID: 34680114; PMCID: PMC8533414

Gómez-Sequeda N., Cáceres M., Stashenko E.E., Hidalgo W., Ortiz C., 2020. Antimicrobial and Antibiofilm Activities of Essential Oils against *Escherichia coli* O157:H7 and Methicillin-Resistant *Staphylococcus aureus* (MRSA). *Antibiotics* 9(11): 730. https://doi.org/10.3390/antibiotics9110730

Gopinath V., Priyadarshini S., Loke M.F., Arunkumar J., Marsili E., Velusamy P., 2017. Biogenic synthesis, characterization of antibacterial silver nanoparticles and its cell cytotoxicity. *Arabian Journal of Chemistry* 10: 1107–1117. https://doi.org/10.1016/j.arabjc.2015.11.011

Gupta A.K., Tomas E., 2003. New antifungal agents. *Dermatologic Clinics* 21(3): 565–576. https://doi.org/10.1016/S0733-8635(03)00024-X

Hashem A.H., Albader N.M., Khan A.Q., F. O. Alotibi, A. Al-Askar, A… Elbahnasawy M. A., 2022. Antifungal Activity of biosynthesized silver nanoparticles using cell-free extract of *Bacillus thuringiensis* against *Aspergillus* species. *Journal of Functional Biomaterials* 2022: 13(4): 242. https://doi.org/10.3390/jfb13040242

Jung K.W., Chung M.S., Bai H.W., Chung B.Y., Lee S., 2021. Investigation of Antifungal Mechanisms of Thymol in the Human Fungal Pathogen, *Cryptococcus neoformans*. *Molecules* 26(11): 3476. https://doi.org/10.3390/molecules26113476

Kanika C. and Satyawati S., 2022. Chemical composition, antioxidant and antifungal activity of essential oil of *Trachyspermum ammi* seeds. *International Journal of Advanced Research* 10(4): 592–596.

Khader M. and Eckl P.M., 2014. Thymoquinone: an emerging natural drug with a wide range of medical applications. *Iranian Journal of Basic Medical Science* 17(12): 950–957.

Livak K.J. and Schmittgen T.D., 2001 Analysis of relative gene expression data using real-time quantitative PCR and the 2$^{-\Delta\Delta CT}$ method. *Methods* 25: 402–408.

Machado F.J., Santana F.M., Lau D., Ponte E.M., 2017. Quantitative review of the effects of triazole and benzimidazole fungicides on Fusarium head blight and wheat yield in Brazil. *Plant Disease* 101(9): 1633–1641. https://doi.org/10.1094/PDIS-03-17-0340-RE

Mallmann E.J., Cunha F.A., Castro B.N., Maciel A.M., Menezes E.A., Fechine P.B., 2015. Antifungal activity of silver nanoparticles obtained by green synthesis. *Revista do Instituto de Medicina Tropical de São Paulo* 57(2): 165-167. https://doi.org/10.1590/S0036-46652015000200011. PMID: 25923897; PMCID: PMC4435016.

Mossa M.I., El-Sharkawy E.E., ElSharawy A.A., 2023. Antifungal activity of silver nanoparticles green biosynthesis from the extract of *Zygophyllum album* (L.f.) on Fusarium wilt. *Journal of Plant Protection Research* 63(3): 340–349. https://doi.org/10.24425/jppr.2023.146874.

Peng Z., Chen, L., Zhu, Y., Huang, Y., Hu, X.,... Yang W., 2018. Current major degradation methods for aflatoxins: A review. *Trends in Food Science & Technology* 80: 155–166. https://doi.org/10.1016/j.tifs.2018.08.009

Pirbalouti M.A., Shahbazi S., Shahrokh S.S., Reiisi S., Mokhtari A., 2024. Study the antifungal effects of green synthesized silver nanoparticles on the *Aspergillus niger*, *Microsporum canis*, and *Candida albicans*. *Journal of Microbiota* 1(3): e154535. https://doi.org/10.5812/jmb-154535

Vanlalveni C., Ralte V., Zohmingliana H., Das S., Anal J.M.H., ... Rokhum S.L., 2024. A review of microbes mediated biosynthesis of silver nanoparticles and their enhanced antimicrobial activities. *Heliyon* 10(11): e32333. https://doi.org/10.1016/j.heliyon.2024.e32333

Vignesh A., Menaka C., Amal T.C., Selvakumar S., Vasanth K., 2025. Exploring the dual impact of nanoparticles on human well-being: A comprehensive review of risks and benefits. *Next Nanotechnology* (8): 100223. https://doi.org/10.1016/j.nxnano.2025.100223

Vijayakumar S., Malaikozhundan B., Shanthi S., Vaseeharan B., Thajuddin N., 2021. Biological compound

capping of silver nanoparticles with the seed extracts of black cumin (*Nigella sativa*): a potential antibacterial, antidiabetic, anti-inflammatory, and antioxidant. *Journal of Inorganic and Organometallic Polymers and Materials* 31: 624–635. https://doi.org/10.1007/S10904-020-01713-4

Wu S., Zhang Q., Zhang W., Huang W., Kong O., ... Yan S., 2022. Linolenic Acid-Derived Oxylipins Inhibit Aflatoxin Biosynthesis in *Aspergillus flavus* through Activation of Imizoquin Biosynthesis. *Journal of Agricultural and Food Chemistry* 70(50): 15928–15944. https://doi.org/10.1021/acs.jafc.2c06230

Zakaria L., 2024. An overview of *Aspergillus* species associated with plant diseases. *Pathogens* 20: 13(9): 813. https://doi.org/10.3390/pathogens13090813. PMID: 39339004; PMCID: PMC11435247.